Reports in Mechanical Engineering
Vol. 7, No. 1, 2026, pp. 133-151
ISSN: 2683-5894, DOI: https://doi.org/10.31181/rme551

Multistable Laminated Lattice Unit Cell Structure for Energy Absorption

Adnan Ahmed[1], Samir Emam[1*]
[1]Department of Mechanical Engineering, American University of Sharjah, Sharjah, PO Box 26666, United Arab Emirates

Article Info

Article history:

Received February 9, 2026
Revised March 11, 2026
Accepted March 20, 2026

Keywords:

Lattice Structure,
Bistable Laminates,
Impact Analysis,
Auxetic Structures,
FE Modeling

ABSTRACT

Reconfigurable structures offer tunable mechanical response through easy switchability among their stable configurations. Bistable hybrid laminates have shown to be great candidates as constituent material in morphing structures offering two stable shapes for various boundary conditions. The bistability stems from the vastly different coefficients of thermal expansion upon cooling the laminate to the room temperature. A reconfigurable lattice structure exhibiting multiple stable shapes without the need of a holding force or continuous supply of energy would be extremely useful and desirable in certain applications. In this study, an innovative lattice unit cell structure made of hybrid bistable laminates is proposed to offer a tunable mechanical response and vastly different Poisson's ratio among the different stable configurations when used as a repeating unit in a large lattice structure. A detailed FE model using ABAQUS® is presented which is used to analyze the multiple stable shapes of the unit cell and their mechanical response under impact loading. Each shape can be achieved easily through simple snap through processes yet exhibit substantial difference in energy absorption capability. This study explores a new area of research in designing laminated lattice structures which are tunable according to the desired application owing to multiple stable shapes.

Corresponding Author:

Samir Emam
Department of Mechanical Engineering, American University of Sharjah, Sharjah, PO Box 26666, United Arab Emirates
Email: semam@aus.edu

1. Introduction

Morphing structures possess the ability to modify their shape in response to changing conditions, thereby enhancing their multifunctional performance. Owing to their capacity to achieve multiple stable configurations, multistable structures have emerged as promising candidates for morphing applications in various adaptive systems (Deshpande et al., 2024; Pan et al., 2020). Multistability can be induced through different means, such as utilising the differential thermal expansion coefficient in fibre-reinforced composite laminates (Hyer, 1981b; Liu et al., 2023; Liu et al., 2024), incorporating geometric features such as initially curved shells (Kuang et al., 2021), origami and kirigami concepts (Yang et al., 2018), or by applying prestressing (Daynes et al., 2008). Their capability to transition between distinct shapes or configurations, while maintaining stability in each configuration provides significant versatility for designing adaptive and morphing systems that can dynamically respond to environmental variations or operational requirements. A detailed review of different bistable and multistable mechanisms, emphasizing their structural concepts, materials, and functionalities, is presented by Chi et al. (Chi et al., 2022).

Rafsanjani and Pasini (Rafsanjani & Pasini, 2016) used ancient geometric motifs as an inspiration to create bistable auxetic metastructure with square and triangular grids. Their design consisted of a network of rotating units connected by compliant hinges, which achieved simultaneous auxeticity and bistability. Chen et al. (Chen et al., 2021) extended the work of Rafsanjani and Pasini (Rafsanjani & Pasini, 2016) to develop a computational solution for the inverse design of the metastructure that would conform to complex 3D shapes while maximizing the bistability as well as stiffness of the cell to ensure robust deployment. Haghpanah et al. (Haghpanah et al., 2016) introduced a novel class

of multistable architected metastructures incorporating active hinges, enabling large shape transformation through snap-through mechanism. However, their design's feasibility is found to be contingent on the failure strain of the hinged material. Their investigation revealed that diminishing the unit cell size could generate hinges capable of undergoing snapping behavior without experiencing plastic deformation, thereby yielding more efficient multistable configurations. In another study, Rafsanjani et al. (Rafsanjani et al., 2015) presented a mechanical metamaterial consisting of a periodic arrangement of snapping units capable of tunable tensile behavior when subjected to tension, the metamaterial exhibits significant extension due to sequential snap-through instabilities, resulting in a transition from an undeformed wavy-shape to a diamond configuration. Shan et al. (Shan et al., 2015) devised an architectured material constructed from inclined beams exhibiting bistability, suitable for energy trapping applications. The mechanism solely arises from structural geometry and is independent of material and load rate. The bistable shape response of inclined beams could be tailored by modifying its geometric parameters such as length, depth and its inclination angle. Importantly, the loading process exhibited reversibility, enabling the structure to be reused multiple times without compromising its energy absorption capacity. This design holds significant potential for applications in areas such as personnel protection, crash mitigation, and protective packaging. Such concepts have been extensively extended to achieve shape adaptive metastructures, especially from printed materials (Chen et al., 2021; Y. Zhang et al., 2020). Risso et al. (Risso et al., 2022) developed a metastructure exhibiting multistability constructed using four identical strips with an equi-biaxially stretched soft membrane. The response of such metastructure could be tailored through variations in the strip material and geometrical parameters.

Several concepts of multistable metastructures have also been explored by folding and cutting using techniques using origami and kirigami (Yang et al., 2018; Yasuda & Yang, 2015; Zhang et al., 2022). All these works have demonstrated significant shape-adaptivity but are not designed to carry significant loads, which is often desired in morphing applications (Daynes & Weaver, 2013). In the recent past, multistability has been engendered in fibre-reinforced composites to satisfy conflicting requirements in a morphing application, which is to be lightweight, shape adaptive, and load-carrying at the same time (Haldar et al., 2020; Lachenal et al., 2013). In isotropic materials, multistability can be induced by changing various geometrical properties such as initial curvature (Kebadze et al., 2004), prestressing, topological and geometrical changes via kirigami concepts (Yang et al., 2018), folds (Waitukaitis et al., 2015) and surface patterns (Udani & Arrieta, 2021). The combination of both programming the geometry and the material anisotropy has resulted in diverse stable shapes (Haldar et al., 2018) and has been found to exhibit tristability in certain cases (Coburn et al., 2013; Vidoli & Maurini, 2008).

A classic example of multistability is observed in the bistable behavior of unsymmetrical composite laminates. Such laminates exhibit two distinct stable configurations at ambient temperature because of residual thermal stresses induced during the curing process (Hyer, 1981b).

To use these unsymmetric laminates for any practical application, it is required to integrate them as a part of a larger structure. The unsymmetric laminates which are studied in the literature (Hyer, 1981a, 1981b), loses bistability when clamped. In all these attempts, there has been a very limited study on the modeling of the composite laminates as a part of a larger compliant structure in any boundary conditions other than free-free. To obtain a clampable bistable laminate, Mattioni et al. (Mattioni et al., 2009) proposed a piecewise layup comprising of a symmetric and an unsymmetric section that could be clamped at one end. As a possible application of these bistable laminates, Bilgen et al. (Bilgen et al., 2013) demonstrated that the laminate could be snapped between the two equilibrium states via dynamic actuation by piezoelectric patches attached to laminate surface. Furthermore, it was shown that the two configurations exhibit distinct aerodynamic characteristics while possessing sufficient stiffness to sustain the shapes under aerodynamic loading. Li et al. (Li et al., 2014) proposed a clampable metal hybrid symmetric laminate that has two symmetric cylindrical stable configurations where they used an analytical model to obtain the two stable equilibrium shapes of the proposed layup in the free-free boundary condition. Mukherjee et al. (Mukherjee et al., 2020) modified the metal hybrid laminate by replacing the aluminum layers in the layup by glass-epoxy bi-directional (BD) plies. It has been shown that this modification in the layup largely eliminates the problem of slippage and debonding between the metal and the carbon-epoxy layers. The improvement in the bond strength between the glass-epoxy and the carbon-epoxy layers has been demonstrated in the manuscript by performing lap shear tests on standard manufactured specimen. Recently, Hijazi and Emam (Hijazi & Emam, 2023) studied the effect of the BD plies' thickness, width, and location from the laminate's centerline on the stable shapes and the snapthrough behavior of a clamped hybrid bistable laminate.

Lattice structures are periodic porous materials composed of repeating unit cells arranged in defined patterns. Nature demonstrates the use of lattice structures for example, the FCC lattice of NaCl, BCC metallic crystals, the trabecular architecture of bones and plant stems, and the 2D honeycomb built by bees. Owing to their excellent

strength-to-weight ratio, energy absorption, thermal insulation, noise damping, and lightweight properties (Liu et al., 2019; Nagesha et al., 2020), lattice structures are used across diverse fields such as mechanical, civil, automotive, aerospace, defense and biomedical engineering (Feng et al., 2021; Khosroshahi et al., 2018; Spadoni & Ruzzene, 2007; Wang et al., 2018). In recent times, lattice structures and their applications have gained much interest and attention in the mechanical engineering and structural engineering fraternity. Lattices are broadly classified into 2D and 3D lattices. 2D lattices include honeycombs, auxetic lattices, and hierarchical 2D lattices. Honeycombs remain the most studied 2D lattice for their superior energy absorption. Auxetic lattice structure is the class of structures that exhibits negative Poisson's ratio which includes re-entrant honeycombs. 3D lattices include truss-based (Nečemer et al., 2020; Tancogne-Dejean & Mohr, 2018), plate-based (Berger et al., 2017; Tancogne-Dejean et al., 2018), shell-based (Yin et al., 2020; Zhao et al., 2020), and hierarchical types (Zhang et al., 2021; Zheng et al., 2016). Energy-absorption studies commonly consider compression (Kucewicz et al., 2019), tension (Jiang & Wang, 2016), bending (L. Zhang et al., 2020), torsion (Jiang & Wang, 2016), shear (Feng et al., 2017), and combined loadings (Zhang et al., 2019). For 2D lattices, out-of-plane compression typically provides higher energy absorption than in-plane loading (Khan et al., 2012).

The compression response generally includes elastic, plastic, and densification stages. Lattices are fabricated from metals, polymers, ceramics, and composites (Deshpande et al., 2001; Kooistra & Wadley, 2007; Queheillalt et al., 2008; Wang et al., 2010). The use of laminated composites is gaining popularity for manufacturing lattice structures in energy absorption applications. Shape-changing laminated structures can change their morphology and mechanical properties, including origami-inspired deployable/foldable laminated structures (Ahmed et al., 2024) and multistable laminated structures. Origami-inspired deployable/foldable laminated structures can be designed using a combination of stiff and flexible materials to introduce desired flexibility (Ahmed et al., 2024) but they are not good in absorbing energy applications. Lattice structures can be made using multistable laminated structures that can exhibit energy absorption capabilities which are tunable due to the multistable configuration of individual unit cells. The shape of the lattice structures can be changed mechanically through application of force or by using smart materials which respond to thermal changes, electric potential, or electromagnetic (EM) fields. Integration of these smart materials with innovative structural designs creates synergistic systems with enhanced functionality and performance. Laminated lattice structures offer several advantages over conventional lattice structures due to the combination of fiber-reinforced composite laminates with lattice geometries. They provide significantly higher specific strength and stiffness because composites possess superior strength-to-weight and stiffness-to-weight ratios. In addition, their mechanical properties can be tailored by adjusting the fiber orientation, stacking sequence, and laminate thickness, allowing precise control of anisotropic behaviour compared with conventional lattices that rely mainly on geometry and base material.

Laminated lattices also exhibit improved energy absorption through progressive damage mechanisms such as matrix cracking, fiber breakage, and delamination. Furthermore, they can incorporate integrated or jointless hinges that reduce stress concentrations typically present at node connections in traditional lattices. The use of multistable laminates in manufacturing lattice structures is less explored relatively new area of research. Using multistable laminates to manufacture lattice structures, provide additional advantages such as the ability to switch between multiple stable configurations without continuous external energy input, enabling shape reconfiguration, deployability, and compact storage. This multistability also improves structural adaptability, vibration isolation, and energy absorption capability, making these structures particularly suitable for lightweight adaptive systems and advanced engineering applications.

In the present study, we propose an innovative lattice unit cell made of hybrid bistable laminates, capable of energy absorption during impact loading and tunable mechanical response. A simple square pristine unit cell can be switched to multiple stable configurations which can be approximated as honeycombs, re-entrant honeycombs and semi reentrant honeycombs exhibiting, positive Poisson's ratio, negative Poisson's ratio and zero Poisson's ratio, respectively. The three stable shapes shall exhibit different mechanical response and performance when used in a large lattice structure but will have identical performance when single cell is evaluated. To demonstrate different behavior and response at cell level, we have analyzed dual rib and triple rib unit cells and compared the performance in comparison with single rib unit cells. A detailed FE model is presented to analyze the performance of all cases of the unit cell. The three stable configurations are shown to be easily switchable through a snap through process. An impact analysis is also performed for three values of impact velocities demonstrating the energy absorption performance for the three stable configurations of the dual rib and triple rib unit cell.

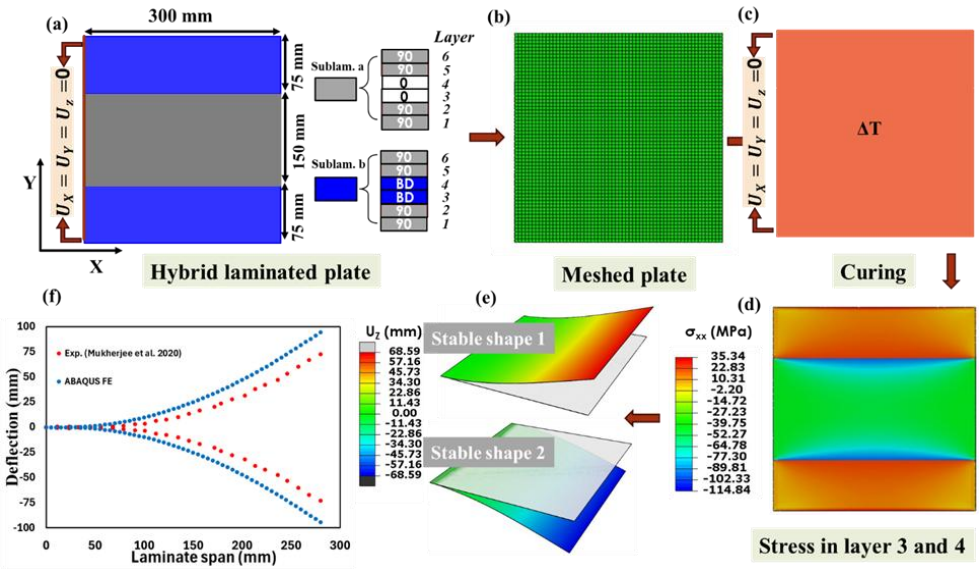

Figure 1: (a)-(e) FE Modeling Steps to Demonstrate Bistable Behavior of Hybrid Laminated Cantilever Plate (F) Validation with Experimental Results

2. Design and FE Model

2.1 Bistability of a Hybrid Laminated Plate

The bistability in a hybrid laminate has been demonstrated in several studies through experimental or analytical analysis where it is shown that the multiple shapes are achieved through various activation and mechanisms as discussed in introduction. In our context the mechanism responsible for achieving multiple stable shapes is the vast difference in the thermal coefficients of adjacent laminas indicated by the materials properties given in Table 1. An FE model is presented to demonstrate the mechanism of bistability in hybrid laminated plate with cantilever boundary conditions.

Table 1: Material Properties of Constituent Laminas

Material Property	E_1 (GPa)	E_2 (GPa)	v_{12}	E_{12} (GPa)	$\alpha_1(10^{-6}/°C)$	$\alpha_2(10^{-6}/°C)$
UD Carbon Epoxy	137.4	10.07	0.23	4.4	0.37	24.91
BD Glass Fabric Epoxy	22.3	22.3	0.20	4.75	19.78	19.78

The steps for FE modeling and stable shapes for demonstrating bistability is shown in Figure 1. A square hybrid laminated plate of side 300 mm is modeled using 3D part modeling which requires modeling of each layer separately along the thickness direction. The hybrid laminated plate has six layers of 0.125 mm each where stacking scheme for sub-laminate (a) is $[90_2/BD_2/90_2]$ and for sublaminate (b) is $[90_2/0_2/90_2]$. The widths of each sublaminate are shown in Figure 1. The modeling is followed by meshing using 3D stress element C3D20R where each element has a size of 5 mm × 5 mm × 0.125 mm. The size of each element considered here is selected after a mesh convergence study in which the size is selected if the next smaller element size shows equal values of stresses up to two decimal places. The use of 3D element is preferable in this scenario where we need to obtain inplane stress at each layer without the assumptions of shell elements. As shown in Figure 1 (a), after meshing, the cantilever boundary conditions and the temperature variation are applied on the hybrid plate.

In the first analysis step the temperature change which is applied using predefined field in ABAQUS is changed from 150 ºC to 30 ºC resulting in compressive and tensile inplane stresses (σ_{xx}) existing simultaneously in the same plane in layers 3 and 4 (Figure 1 (d)). This results in the initiation of buckling. In the next step we applied a load in positive or negative normal direction on the tip of the cantilever plate and subsequently removed it to obtain the two stable shapes as shown in Figure 1 (e). To validate the FE model and results we have compared the experimental results of Mukherjee et al. (Mukherjee et al., 2020) and compared with FE results using the present FE model in Figure 1 (f). There is a good agreement between the experimental and FE results for the hybrid plate considered in the reference study (Mukherjee et al., 2020). In the next section the bistable hybrid laminated plate is used as the repeating

part to obtain a multi stable unit cell structure.

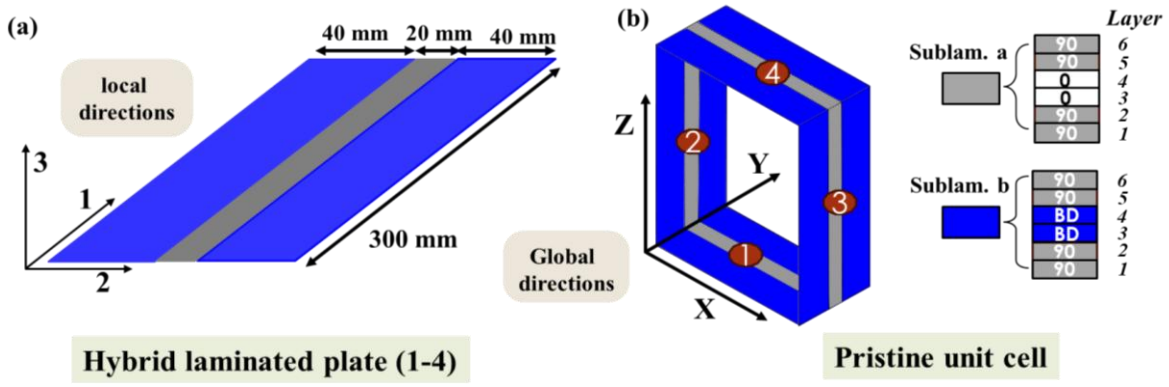

Figure 2: A Unit Cell Structure (a) A Single Hybrid Laminated Plate and (b) A Square Unit Cell as an Assembly of Four Hybrid Laminated Plates with the Laminate Scheme

2.2 Multi-Stable Unit Cell Structure

A multi-stable unit cell (MSUC) structure is proposed here which is square in shape, as shown in Figure 2 (b). The pristine unit cell is fabricated using four identical hybrid laminated plates, each having dimension of 300 mm × 100 mm which are fabricated using two sublaminates having laminas made of unidirectional carbon fiber-epoxy (UD) and bidirectional glass fiber-epoxy (BD) (Table 1). The stacking scheme for sub-laminate (a) is $[90_2/BD/90_2]$ and for sublaminate (b) is $[90_2/0_2/90_2]$. Each of the six layers is 0.125 mm thick. The widths of the constituent laminas are also illustrated in Figure 2 which is selected based on the study of widths of sublaminates a and b resulting in maximum bistability effect for the particular materials, laminate dimension and stacking. This unit cell can be employed in a repeated pattern to form a lattice which can be tailored for desired mechanical behavior owing to the multi-stable configurations possible. It is already shown in the previous section and through other experimental, analytical and numerical analysis (Li et al., 2014; Mukherjee et al., 2020; Zhang et al., 2024) that clamped-free and clamped-clamped symmetric hybrid laminates can demonstrate bistability by using laminas having vastly different coefficients of thermal expansion. In this study a multi-behavior cell structure is proposed and analyzed having three stable configurations easily switchable from one shape to another. These stable shapes are called as negative Poisson's ratio cell (NPRC), zero Poisson's ratio cell (ZPRC) and positive Poisson's ratio cell (PPRC). This capability of changing shapes gives the designers freedom to tune the lattice structure according to desired mechanical response.

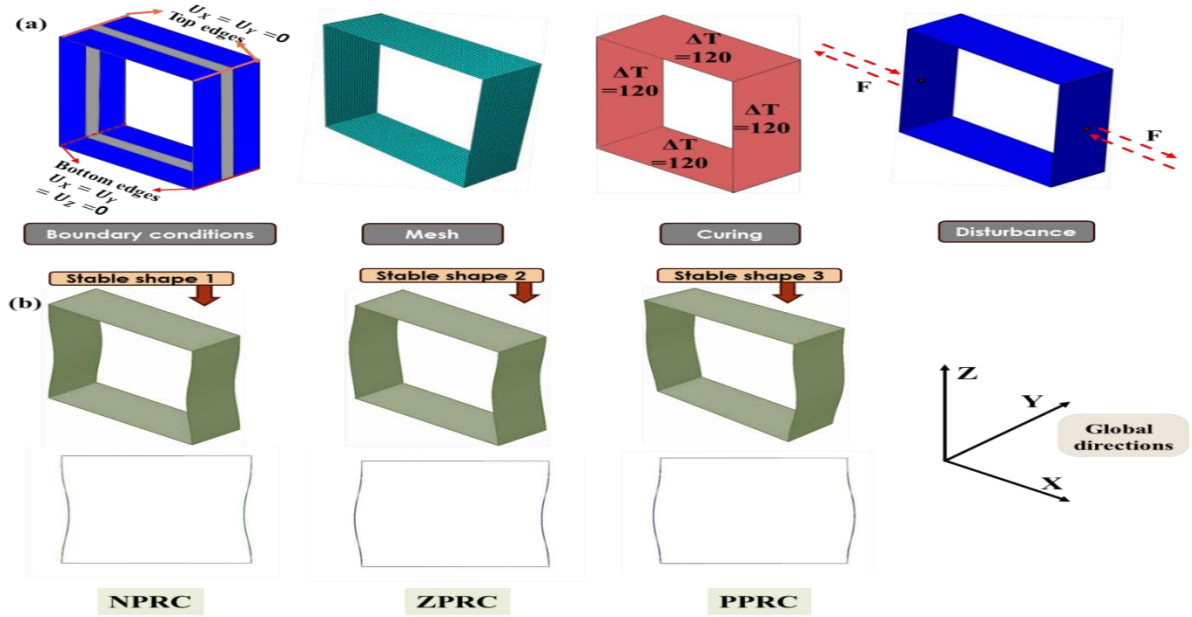

Figure 3: (A) Simulation Steps for Modeling Unit Cells and (B) The Three Stable Configurations of a Unit Cell

The process of obtaining multiple shapes through FE modeling in ABAQUS is demonstrated in the next section.

2.3 FE Model and Poisson's Ratio Estimation of the Unit Cell

The feasibility of the proposed square unit cell for energy absorption application made from bistable laminated plates is assessed here through FE model and analysis. ABAQUS® (2021)/standard is used to model the unit cell and simulate the mechanical response of the multi-stable unit cell. In the part module of ABAQUS, only a hybrid laminated plate is modeled (Figure 1 (a)) which is then used to model the square unit cell in assembly. A composite section is assigned to the hybrid plates with six layers according to the laminate scheme and is meshed with four-node S4R shell elements since, for thin structures shell elements are computationally efficient and accurate when stresses at layer interfaces are not the focus of study. The convergence of mesh density is investigated, and the element size of 5 mm × 5 mm is selected for the study. The total thickness of each hybrid laminated plate is 0.75 mm. The mechanical and thermal properties of constituent laminas are given in Table 1.

The surface was partitioned at the center of the plate to define a strip along the length to define different layups, as shown in Figure 2. The hybrid plate is copied to have four identical parts and used to make a square unit cell in the assembly. Tie constraints are used to connect the four plates at the edges with each other. The 'Nlgeom' (geometrically nonlinear) option is on during the entire analysis process to allow the large deformations.

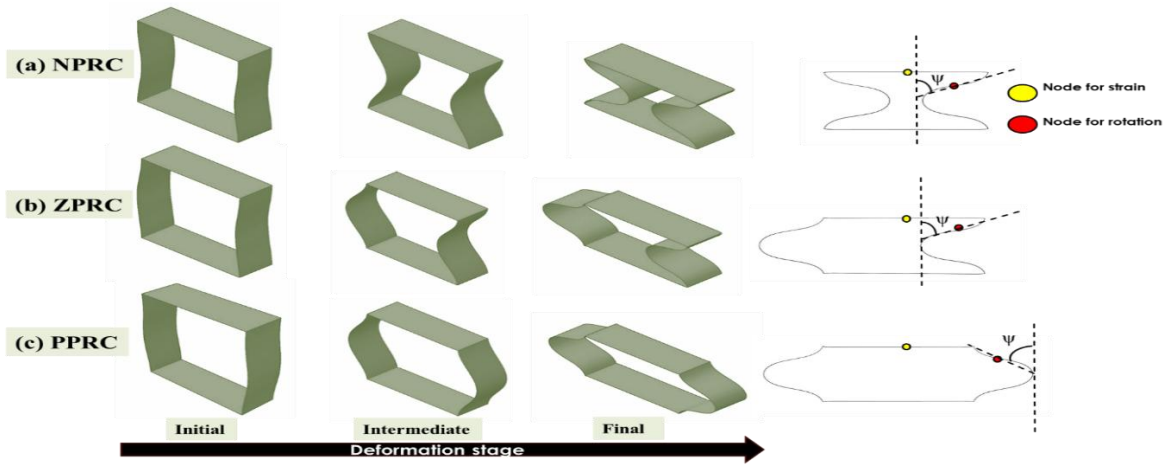

Figure 4: (a) First Stable Shape of the Unit Cell Having Negative Poisson's Ratio, (B) Second Stable Shape Having Zero Poisson's Ratio and (C) Third Stable Shape Having Positive Poisson's Ratio

The dynamic Poisson ratio $v(\psi)$ is given by

$$\nu_{xy}(\psi) = \frac{a}{b+a\sin(\psi)} \times \frac{2(1-\beta^2)\,sin(\psi)cos^2(\psi)}{1+\beta^2-(1-\beta^2)\cos(2\psi)} \quad (1)$$

Where a is the half length of the vertical rib, b is the length of horizontal rib, $\beta = h/a$ and ψ is the angle as shown in Figure 4.

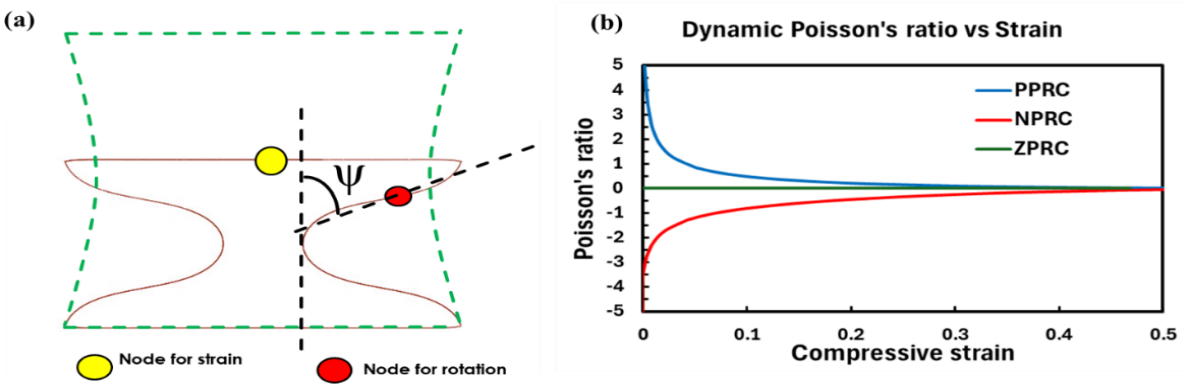

Figure 5: Dynamic Poisson's Ratio Calculation for Unit Cells (a) Rotation of Rib and (b) Poisson's Ratio for NPRC, ZPRC and PPRC

For the present unit cell, $a = 150\ mm, b = 300\ mm, h = 0.75\ mm$, and ψ is taken as the rotation of the node shown in Figure 5 (a) for the unit cells. The dynamic Poisson's ratio v_{xy} depending on the rotation of the curved ribs is shown in Figure 4 (b) which is initially high and negative for NPRC and initially high and negative for NPRC. The value decreases as the compressive strain increases for the unit cells. For ZPRC the Poisson's ratio stays zero for all deformed states.

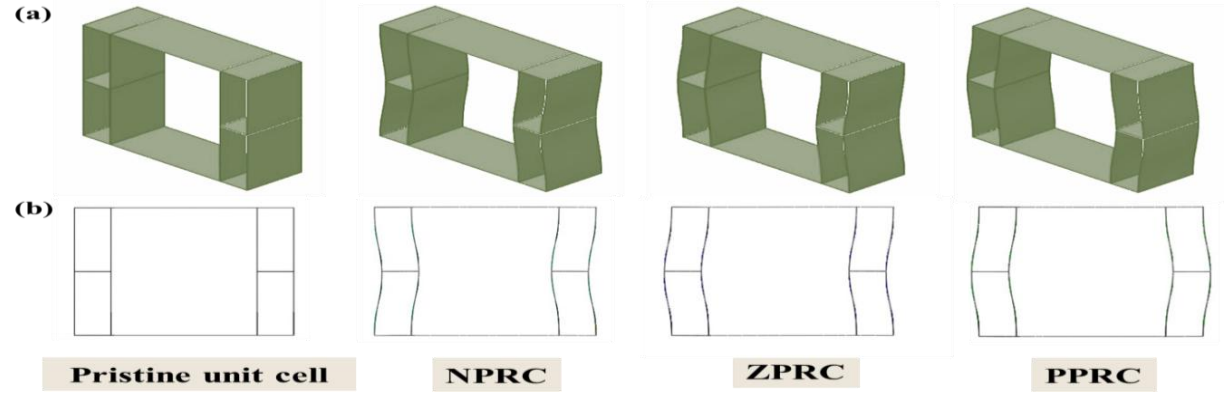

Figure 6: Dual Rib Multi-Stable Unit Cell (a) Isometric View and (b) Front View.

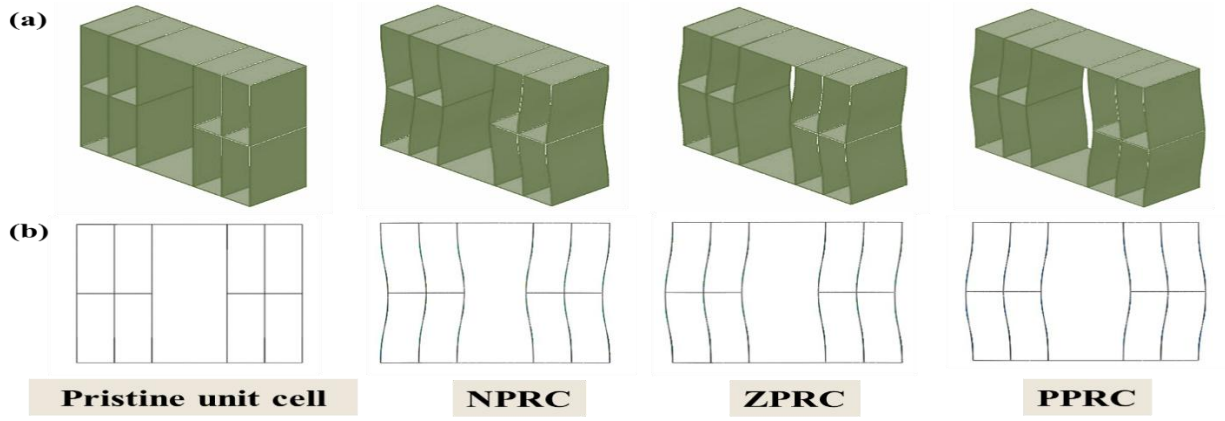

Figure 7: Triple Rib Multi-Stable Unit Cell (a) Isometric View and (b) Front View.

2.4 Dual Rib and Triple Rib Unit Cells

The multi-stable unit cells presented in the previous section exhibit vastly different Poisson's ratio using the same pristine unit cell. They can exhibit different mechanical behavior when used in a lattice, but a single unit cell shows exactly same force-displacement and energy absorption during the deformation since the vertical ribs are experiencing the same path and level of deformation in all three stable shapes. To further enhance the utility and practicality of using multi-stable unit cells, we introduced more vertical ribs in the pristine unit cell as shown in Figures 6 and 7 and will use for analysis of energy absorption capabilities. The vertical ribs are connected to each other through small horizontal ribs enabling snap through from one stable state to the other by applying force on the point\line as done in the single rib unit cell. The boundary conditions are also the same as in the single rib unit cell. After the shape stabilizing step in ABAQUS where the disturbing forces are removed, a dynamic implicit step is added to obtain the response during low to moderate velocity impact on the top rib. Dynamic implicit analysis is employed over the dynamic explicit since it is advantageous for impact simulations, particularly in problems involving low-velocity impacts and moderate nonlinearities. Since the method is unconditionally stable, it allows the use of relatively larger time increments compared with explicit methods, which can reduce the total number of computational steps. It also ensures equilibrium of internal and external forces at each time increment, leading to improved numerical accuracy in predicting structural response. In the present model, a plate having a mass of 2.5 kg is impacted on the top rib having velocity of 10, 20 and 50 m/s for durations of 0.015, 0.075 and 0.003 s, respectively to achieve a compressive strain of 0.5. The surface contact is taken as "Hard contact", and the coefficient of friction is taken as 0.3. The same analysis is also performed on single rib unit cells to have a quantitative comparison among the proposed models

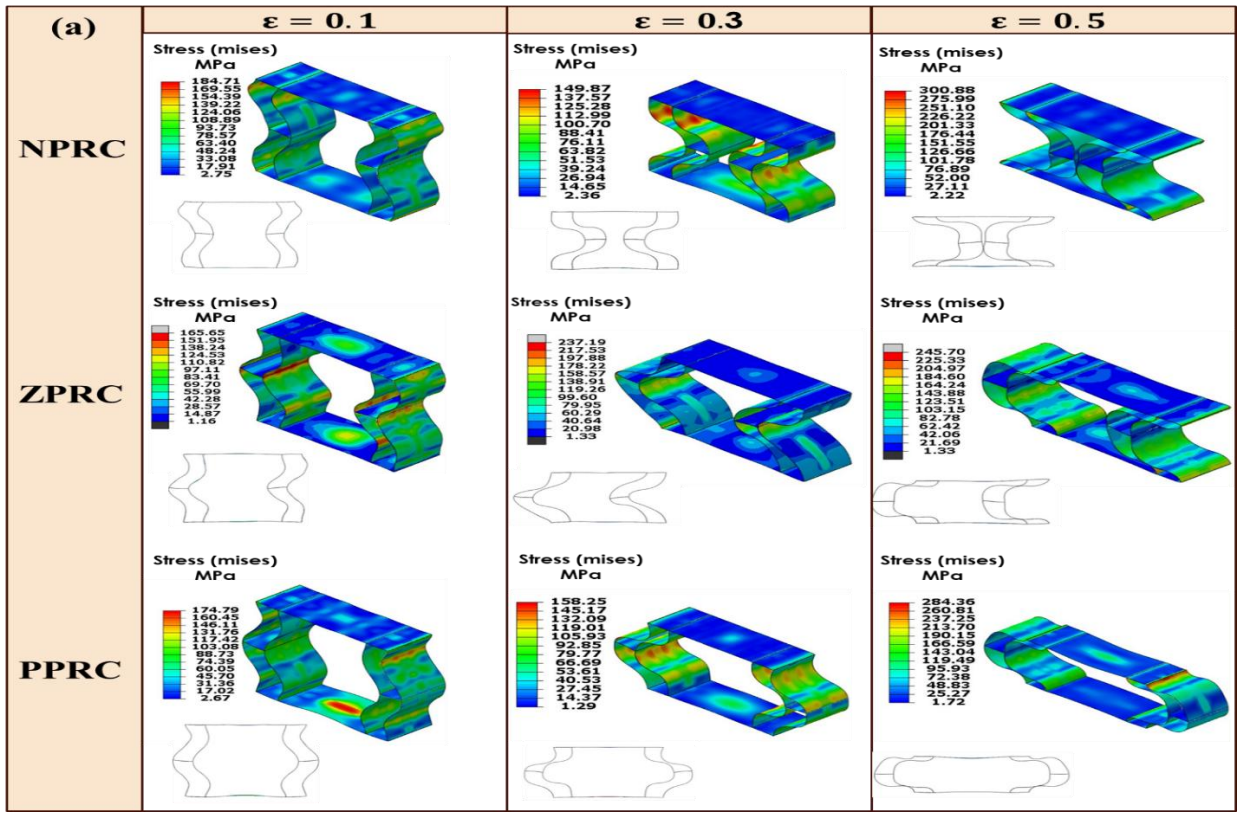
(a)
ε = 0.1
ε = 0.3
ε = 0.5
NPRC
ZPRC
PPRC
Stress (mises)
MPa
184.71
169.55
154.39
139.22
124.06
108.89
93.73
78.57
63.40
48.24
33.08
17.91
2.75
149.87
137.57
125.28
112.99
100.70
88.41
76.11
63.82
51.53
39.24
26.94
14.65
2.36
300.88
275.99
251.10
226.22
201.33
176.44
151.55
126.66
101.78
76.89
52.00
27.11
2.22
165.65
151.95
138.24
124.53
110.82
97.11
83.41
69.70
55.99
42.28
28.57
14.87
1.16
237.19
217.53
197.88
178.22
158.57
138.91
119.26
99.60
79.95
60.29
40.64
20.98
1.33
245.79
225.33
204.97
184.60
164.24
143.88
123.51
103.15
82.78
62.42
42.06
21.69
1.33
174.79
160.45
146.11
131.76
117.42
103.08
88.73
74.39
60.05
45.70
31.36
17.02
2.67
158.25
145.17
132.09
119.01
105.93
92.85
79.77
66.69
53.61
40.53
27.45
14.37
1.29
284.36
260.81
237.25
213.70
190.15
166.59
143.04
119.49
95.93
72.38
48.83
25.27
1.72
(b)
ε = 0.1
ε = 0.3
ε = 0.5
NPRC
ZPRC
PPRC
Stress (mises)
MPa
355.90
325.68
295.46
265.24
245.02
214.80
184.58
154.36
124.14
93.92
63.70
33.48
3.26
307.37
281.90
256.42
230.95
205.47
180.00
154.52
129.04
103.57
78.09
52.62
27.14
1.67
300.88
275.99
251.10
226.22
201.33
176.44
151.55
126.66
101.78
76.89
52.00
27.11
2.22
307.89
282.63
257.38
232.13
206.88
181.62
156.37
131.12
105.86
80.61
55.36
30.11
4.85
544.53
499.46
454.40
409.33
364.26
319.19
274.12
229.06
183.99
138.92
93.85
48.78
3.71
515.21
472.67
430.12
387.58
345.04
302.49
259.95
217.41
174.86
132.32
89.78
47.23
4.69
288.76
265.08
241.40
217.71
194.03
170.34
146.66
122.97
99.29
75.61
51.92
28.24
4.55
369.96
339.49
309.03
278.57
248.10
217.64
187.17
156.71
126.25
95.78
65.32
34.86
4.39
263.26
241.50
219.74
197.98
176.23
154.47
132.71
110.95
89.19
67.43
45.67
23.91
2.15

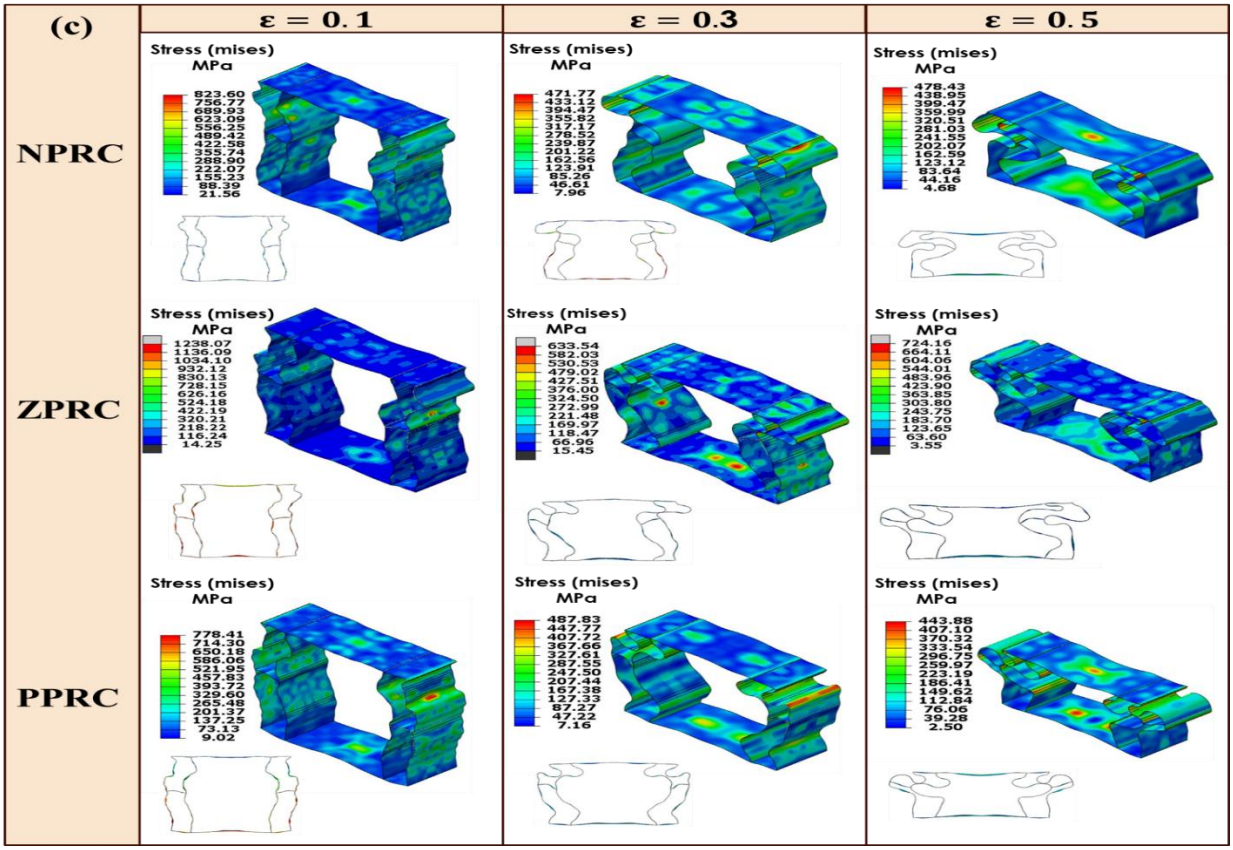

Figure 8: Deformation Modes of Dual Rib Unit Cells for Impact Velocity of (a) 10 m/s, (b) 20 m/s, and (c) 50 m/s

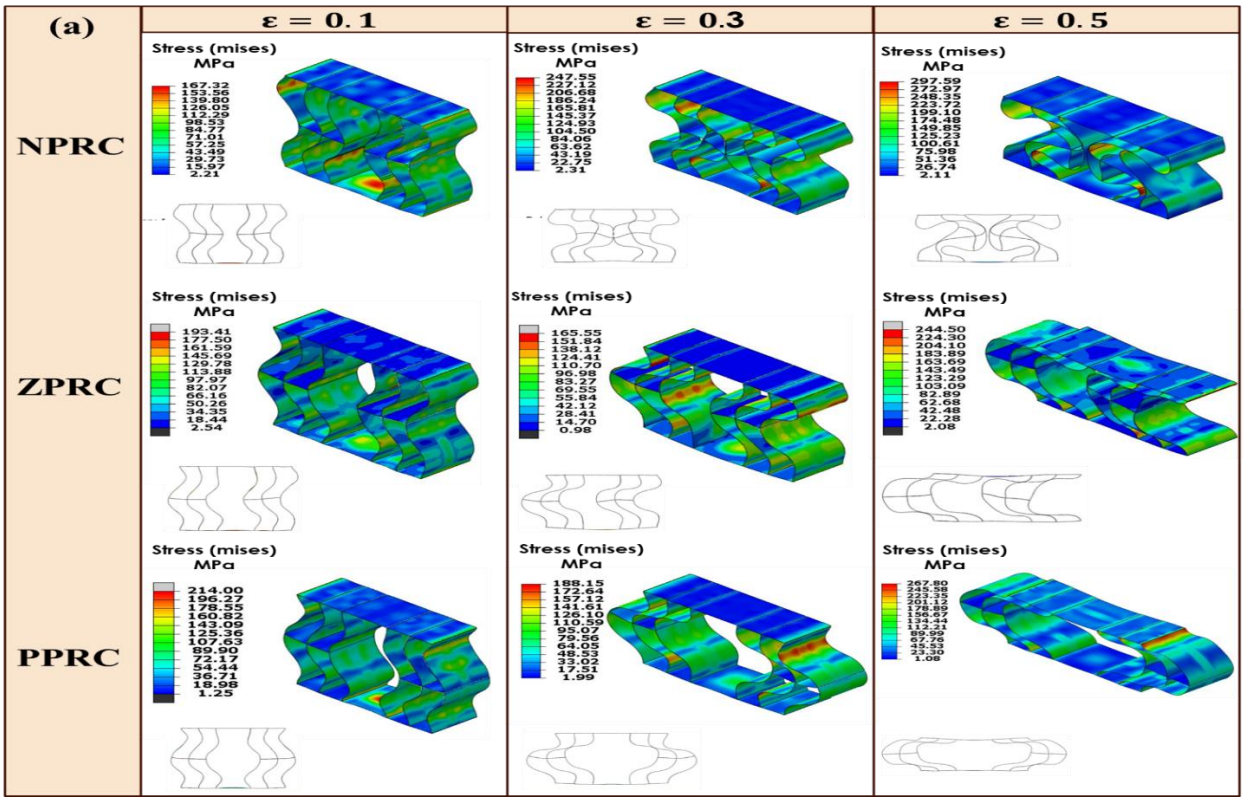

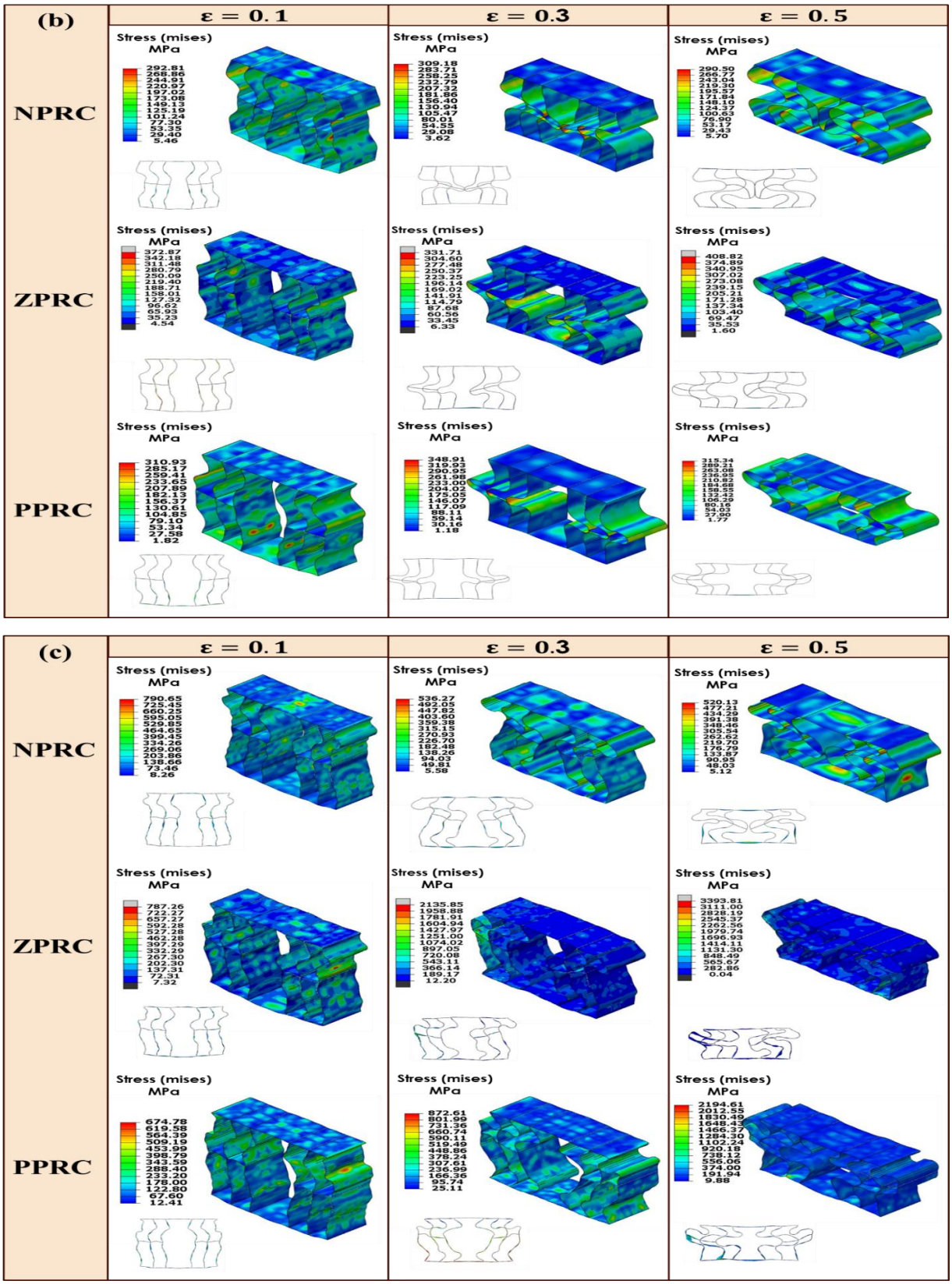

Figure 9: Deformation Modes of a Triple Rib Unit Cells for Impact Velocity of (a) 10 m/s, (b) 20 m/s, and (c) 50 m/s

3. Results and Discussion

3.1 Deformation Pattern of Unit Cells

To assess the performance of the unit cells proposed in the previous section, the energy absorption capabilities of the dual and triple unit cells, a crashworthiness analysis is conducted and compared with each stable shape which can be switched from one to another by a simple snap through process without adding or removing any structural parts. In this section we demonstrate the deformation modes of the dual rib and triple rib unit cells for the three shapes (NPRC, ZPRC, and PPRC). Figures 8 and 9 illustrate the deformation of each of the unit cell shapes and three values of strain when a flat plate of 2.5 kg is impacted at the top rib at different velocities. For low velocity impact on dual rib unit cell the number of pairs of surfaces in contact is similar in all three stable shapes (NPRC, ZPRC and PPRC) for all values of strains. The Von Mises stress is plotted on for the outermost layer to show its variation among the stable shapes and impact velocities. When the impact velocity is moderate i.e. V = 20 and 50 m/s, slightly higher degrees of surface contact are observed in ZPRC unit cells in comparison with PPRC and NPRC. Similarly for triple rib unit cell, ZPRC shape shows much more surface area in contact internally in comparison with NPRC and PPRC when impact velocity is low and strain is low. For moderate velocity impact the surfaces in contact have much larger area in contact. In general, each case is unique showing a unique deformed shape and interaction of internal surfaces with each other.

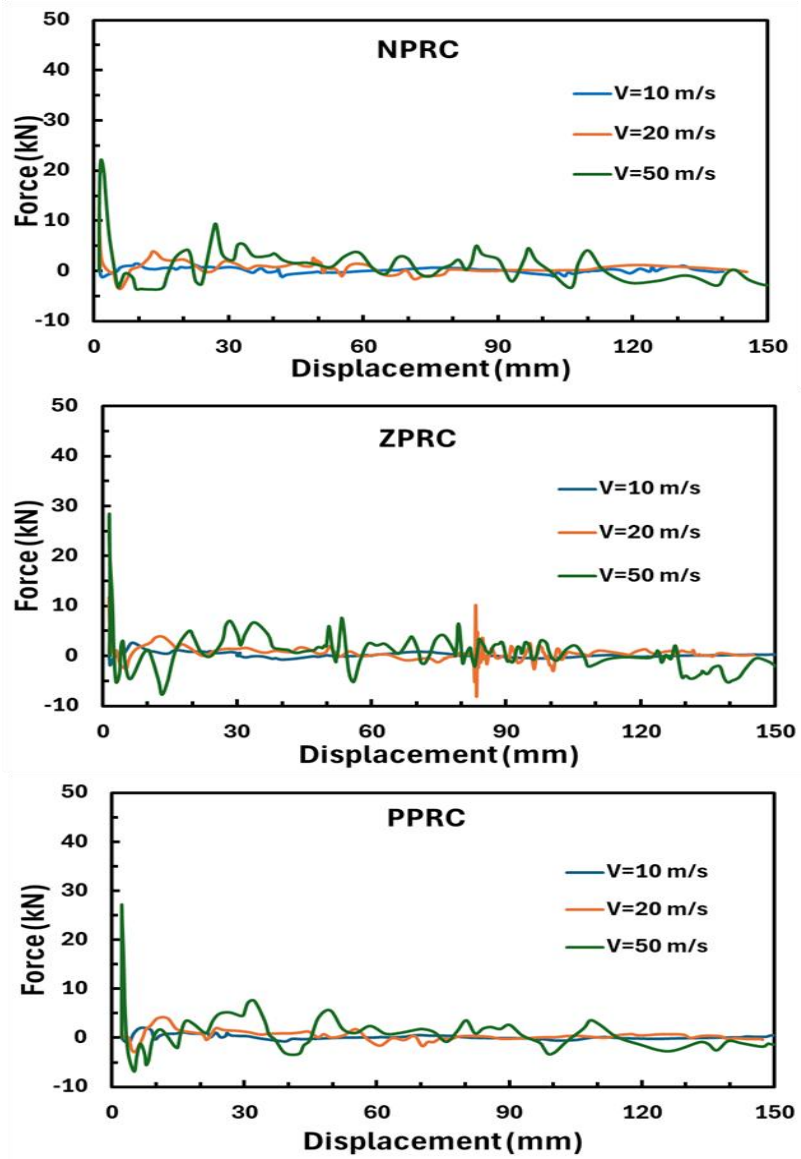

Figure 10: Force Vs Displacement for the Dual Rib Unit Cell Under Various Impact Velocities

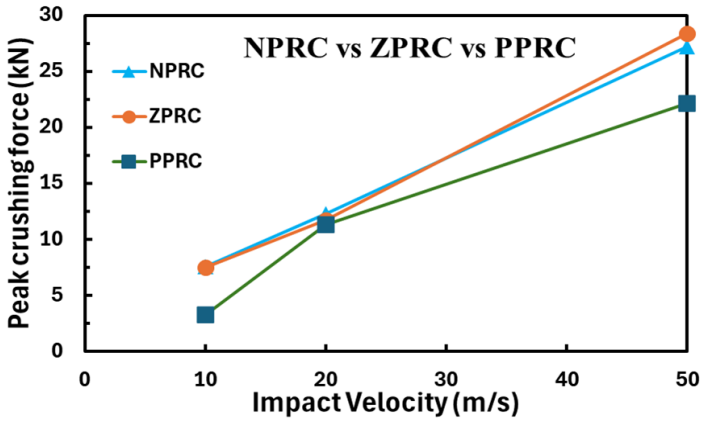

Figure 11: Peak Crushing Force for Dual Rib NPRC, ZPRC and PPRC Under Various Impact Velocities

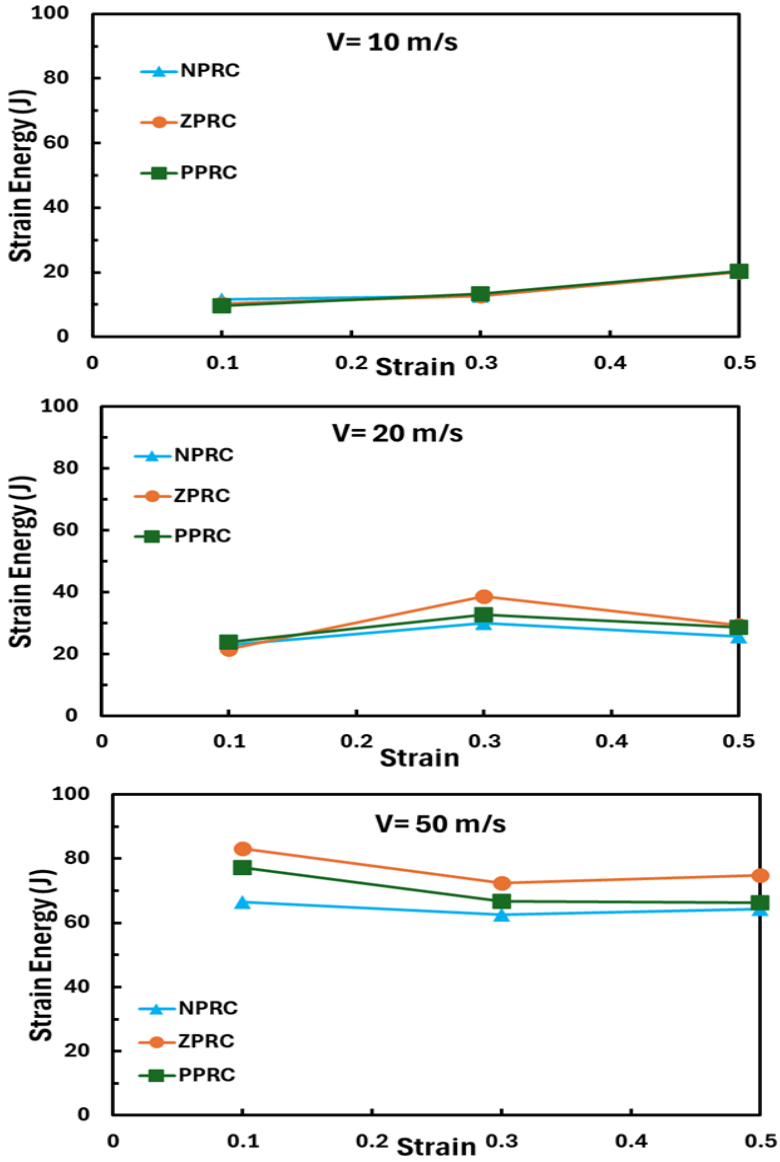

Figure 12: Strain Energy for Dual Rib NPRC, ZPRC and PPRC Under Various Impact Velocities

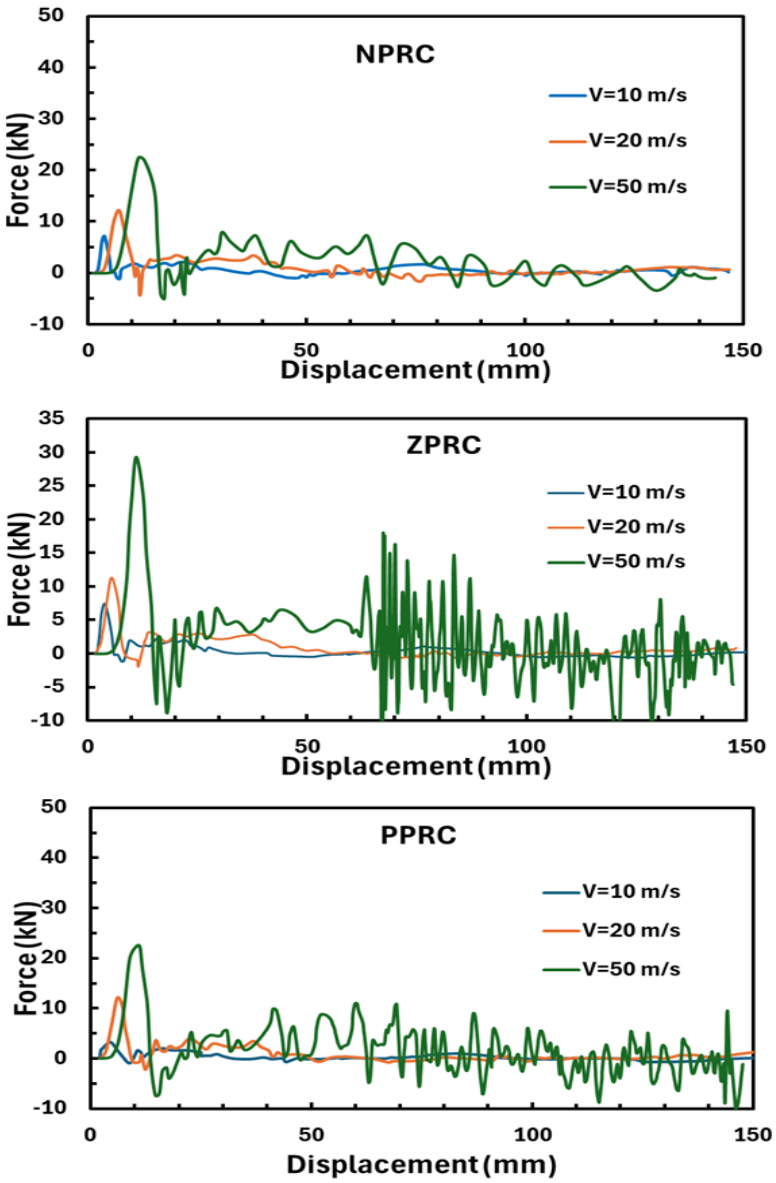

Figure 13: Force vs Displacement for the Triple Rib Unit Cell Under Various Impact Velocities

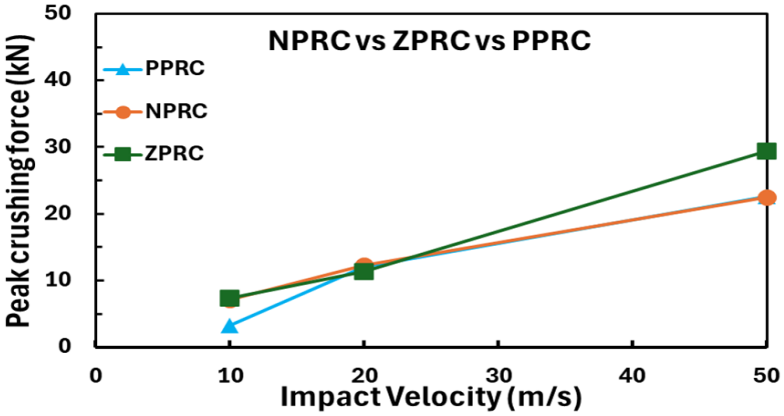

Figure 14: Peak Crushing Force for Triple Rib NPRC, ZPRC and PPRC Under Various Impact Velocities

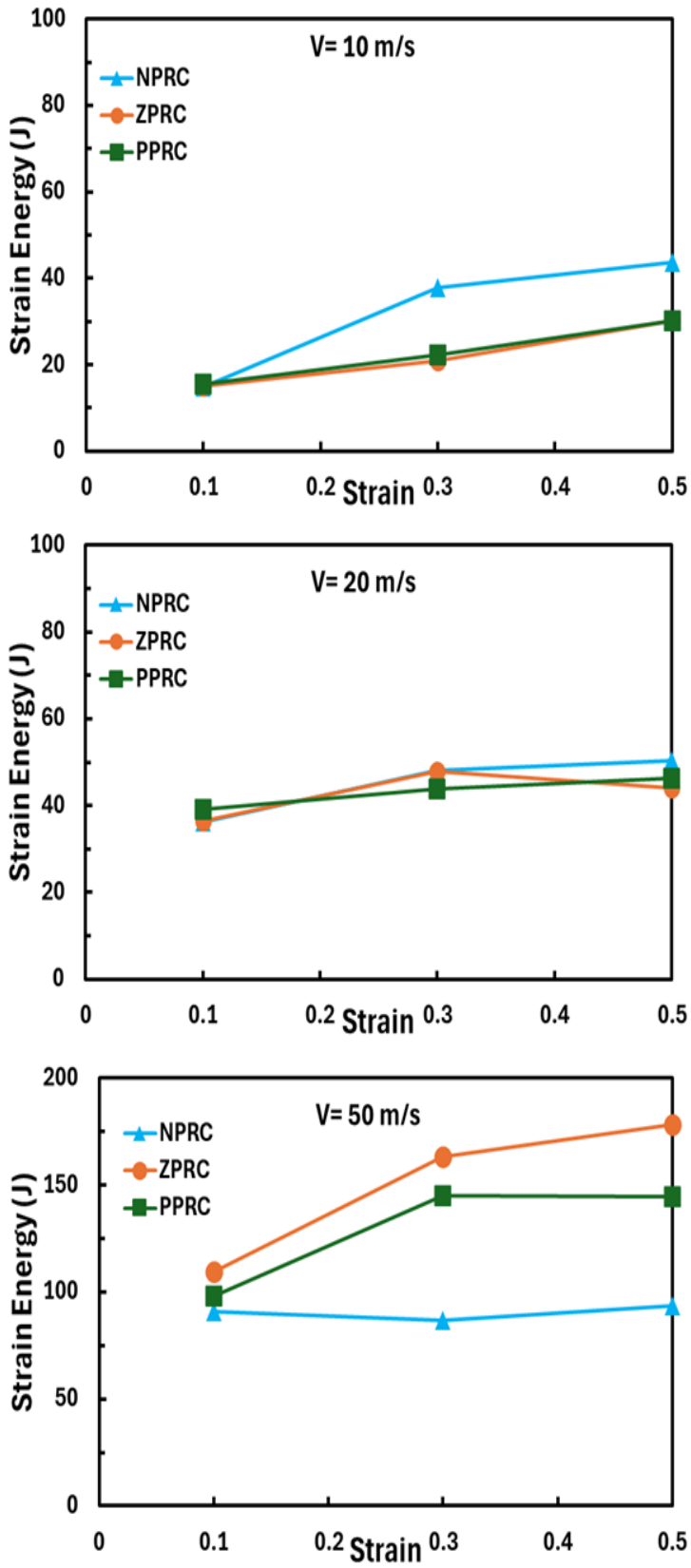

Figure 15: Strain Energy for Triple Rib NPRC, ZPRC and PPRC Under Various Impact Velocities

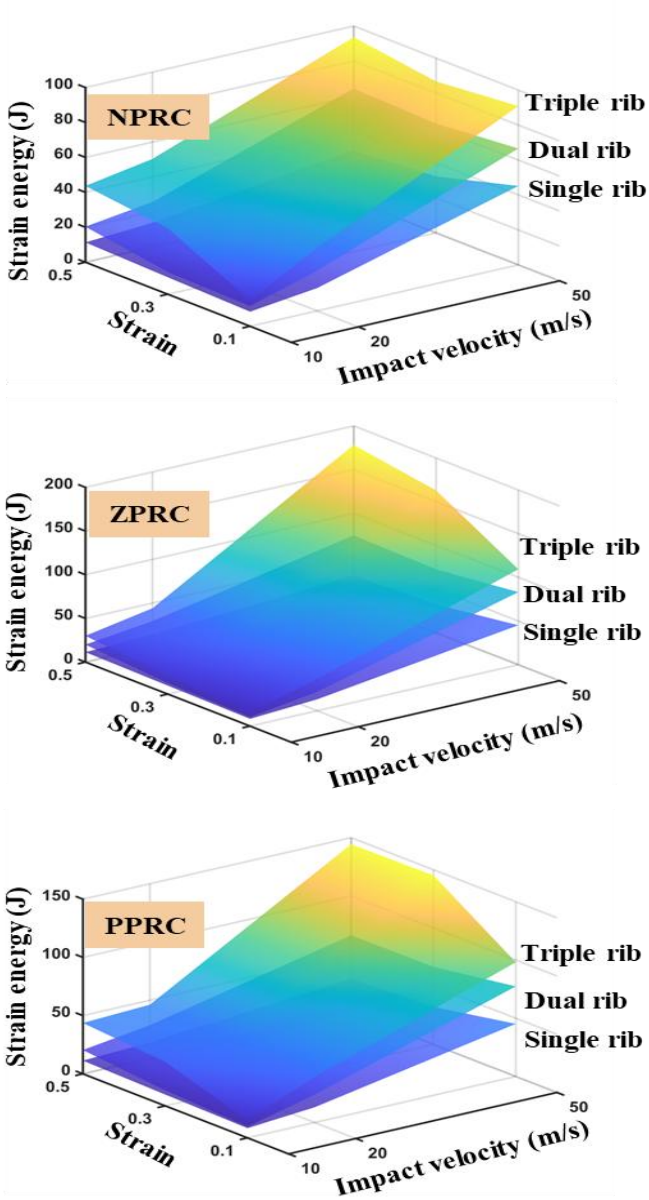

Figure 16: Comparison of Strain Energy Absorbed During Impact for the Single Rib, Dual Rib and Triple Rib Unit Cells vs Strain and Impact Velocity

3.2 Crashworthiness Assessment

Figures 10-15 show the force-displacement curves, the peak crushing force and the corresponding energy absorption curves for NPRC, ZPRC and PPRC under low velocity impact of 10, 20 and 50 m/s for dual rib and triple rib unit cells. The peak crushing force for ZPRC is generally higher than PPRC and NPRC for all velocities when both dual rib and triple rib unit cells are considered. The energy absorbed is also almost same for NPRC, ZPRC and PPRC for low velocity of 10 m/s and low strain of 0.1 for both dual rib and triple rib unit cells whereas for moderate velocities of 20 and 50 m/s, the energy absorbed is not same because the surfaces inside the unit cells interact differently with each other for NPRC, ZPRC and PPRC. The energy absorption characteristics of these unit cells are intricately associated with their deformation modes. It is observed from the deformation profile and energy absorption that a higher degree of surface contact results in higher energy absorption for both dual rib and triple rib unit cells when large deformation occurs at all values of velocities. The peak crushing force, however, doesn't depend on contacting surfaces since it is offered at the initial stage of deformation soon after the impact and only depends on how the structure deforms initially. It is also observed that for higher velocity of the impactor, higher energy is absorbed by

the unit cell. The augmentation of ribs in the unit cells leads to a greater number of folds during deformation, thereby resulting in more contacting surfaces. Consequently, the energy absorption capacity of the unit cell can be enhanced by increasing the number of ribs and varied by selecting among the three stable shapes to fulfill the requirement. To demonstrate the advantage of using multiple ribs in a unit cell over single rib unit cell, a quantitative comparison of energy absorption is shown in Figure 16. The dual rib unit cell would require 58 % more material mass but can enhance energy absorption up to 2.5 times when impact velocity is 20 and 50 m/s. Whereas when triple rib unit cell is employed, 116 % more material mass is added but the energy absorption capability is increased up to 5 times for the impact velocity of 50 m/s.

In addition to the deformed shape, the contact which occurs between surfaces in laminated lattice structures introduces additional contact forces and frictional interactions, which enhance energy dissipation through sliding. Properly defined surface contact prevents unrealistic interpenetration and allows for accurate prediction of deformation modes such as buckling, folding, or progressive collapse. Moreover, contact interactions can promote stress redistribution across the structure, delaying localized failure and increasing the overall energy absorption capacity. However, the effectiveness of energy absorption strongly depends on parameters such as contact stiffness, friction coefficient, and surface definition, as improper contact modeling may either overestimate stiffness or underestimate energy dissipation. Under dynamic/impact loading the internal contact of surfaces are much different from each other among the three stable shapes (NPRC, ZPRC and PPRC) which results in different levels of energy absorption. Introduction of extra parts/ribs in lattice unit cells have been shown to increase energy absorption in hierarchical lattice structures and therefore was expected to improve energy absorption in the proposed design.

Among the three stable shapes studied here, ZPRC exhibits the highest energy absorption in general when both dual rib and triple rib unit cells are considered. The superior energy absorption of ZPRC can be attributed to its shape and interaction of surfaces internally. It is fascinating to see that the same structure but with a ZPRC stable shape can absorb more than double the energy of NPRC at an impact velocity of 50 m/s. This flexibility of enhancing energy absorption capabilities through simple switching of shapes will give designers freedom to tune a lattice structure according to the need.

4. Conclusion

A reconfigurable hybrid laminated unit cell structure is proposed. The unit cell is made of four identical bistable laminates each of two distinct stable shapes. A systematic arrangement of carbon fiber epoxy unidirectional laminas and glass fiber epoxy bidirectional laminas are adopted to induce bistability in the laminate. Through the snapthrough process, three unique configurations of the unit cells can be achieved: honeycomb, reentrant honeycomb and semi reentrant honeycomb structures exhibiting positive Poisson' ratio, negative Poisson's ratio and zero Poisson's ratio. The unit cell can be used as a repeating unit in a larger lattice structure. The three stable configurations of the single rib unit cell are found to have the same stiffness and load-deflection behavior because of the similar deformation patterns and no internal surface interactions. Although, when used in a lattice structure they will affect the structure's overall stiffness differently and show different deformation patterns. In this study, the dual rib and triple rib designs have been shown to perform much better than the single rib unit celland is proposed to further differentiate the mechanical response of each of the configurations at unit cell level and enhance their capability to tune the mechanical response. It is shown that they behave differently through energy absorption capability during impact of three distinct velocities. The deformed shape and energy absorbed for the three configurations are also shown to be substantially different from each other which facilitates the designer to tune the same structure for desired mechanical behavior. In general, the ZPRC configuration for the unit cell exhibits the highest capability for energy absorption among the cases considered in this study. This study opens research opportunities to investigate the possibility of building a lattice structure made of multistable laminated unit cells for energy absorption applications.

References

Ahmed, A., Din, I. U., Kulkarni, S., & Khan, K. A. (2024). Multiscale finite element modeling of origami-inspired dual matrix deployable composite with visco-hyperelastic hinge. *Composite Structures*, *343*, 118301. https://doi.org/10.1016/j.compstruct.2024.118301

Berger, J., Wadley, H., & McMeeking, R. (2017). Mechanical metamaterials at the theoretical limit of isotropic elastic stiffness. *nature*, *543*(7646), 533-537. https://doi.org/10.1038/nature21075

Bilgen, O., Arrieta, A. F., Friswell, M. I., & Hagedorn, P. (2013). Dynamic control of a bistable wing under aerodynamic loading. *Smart materials and structures*, *22*(2), 025020. https://doi.org/10.1088/0964-1726/22/2/025020

Chen, S., Tan, X., Hu, J., Zhu, S., Wang, B., Wang, L., Jin, Y., & Wu, L. (2021). A novel gradient negative stiffness honeycomb for recoverable energy absorption. *Composites Part B: Engineering*, *215*, 108745. https://doi.org/10.1016/j.compositesb.2021.108745

Chi, Y., Li, Y., Zhao, Y., Hong, Y., Tang, Y., & Yin, J. (2022). Bistable and multistable actuators for soft robots: Structures, materials, and functionalities. *Advanced Materials*, *34*(19), 2110384. https://doi.org/10.1002/adma.202110384

Coburn, B. H., Pirrera, A., Weaver, P. M., & Vidoli, S. (2013). Tristability of an orthotropic doubly curved shell. *Composite Structures*, *96*, 446-454. https://doi.org/10.1016/j.compstruct.2012.08.026

Daynes, S., Potter, K., & Weaver, P. (2008). Bistable prestressed buckled laminates. *Composites Science and Technology*, *68*(15-16), 3431-3437. https://doi.org/10.1016/j.compscitech.2008.09.036

Daynes, S., & Weaver, P. M. (2013). Review of shape-morphing automobile structures: concepts and outlook. *Proceedings of the Institution of Mechanical Engineers, Part D: Journal of Automobile Engineering*, *227*(11), 1603-1622. https://doi.org/10.1177/0954407013496557

Deshpande, V., Myers, O., & Li, S. (2024). Large-ratio stiffness switching via harnessing the in-plane buckling and bi-stability of high-load capacity composite laminates. *Composites Part B: Engineering*, *279*, 111440. https://doi.org/10.1016/j.compositesb.2024.111440

Deshpande, V. S., Fleck, N. A., & Ashby, M. F. (2001). Effective properties of the octet-truss lattice material. *Journal of the Mechanics and Physics of Solids*, *49*(8), 1747-1769. https://doi.org/10.1016/S0022-5096(01)00010-2

Feng, J., Liu, B., Lin, Z., & Fu, J. (2021). Isotropic octet-truss lattice structure design and anisotropy control strategies for implant application. *Materials & Design*, *203*, 109595. https://doi.org/10.1016/j.matdes.2021.109595

Feng, L.-J., Xiong, J., Yang, L.-H., Yu, G.-C., Yang, W., & Wu, L.-Z. (2017). Shear and bending performance of new type enhanced lattice truss structures. *International Journal of Mechanical Sciences*, *134*, 589-598. https://doi.org/10.1016/j.ijmecsci.2017.10.045

Haghpanah, B., Salari-Sharif, L., Pourrajab, P., Hopkins, J., & Valdevit, L. (2016). Multistable Shape-Reconfigurable Architected Materials. *Advanced Materials*, *28*(36), 7915-7920. https://doi.org/10.1002/adma.201601650

Haldar, A., Jansen, E., Hofmeister, B., Bruns, M., & Rolfes, R. (2020). Analysis of novel morphing trailing edge flap actuated by multistable laminates. *AIAA journal*, *58*(7), 3149-3158. https://doi.org/10.2514/1.J058870

Haldar, A., Reinoso, J., Jansen, E., & Rolfes, R. (2018). Snap-Through of Bistable Configurations Generated from Variable Stiffness Composites. *Multiscale Modeling of Heterogeneous Structures*, 61. https://doi.org/10.1007/978-3-319-65463-8_4

Hijazi, S., & Emam, S. (2023). An investigation into the static configurations and snapthrough response of clamped hybrid bistable symmetric laminates. *Composite Structures*, *312*, 116880. https://doi.org/10.1016/j.compstruct.2023.116880

Hyer, M. W. (1981a). Calculations of the room-temperature shapes of unsymmetric laminatestwo. *Journal of composite materials*, *15*(4), 296-310. https://journals.sagepub.com/doi/abs/10.1177/002199838101500401

Hyer, M. W. (1981b). Some observations on the cured shape of thin unsymmetric laminates. *Journal of composite materials*, *15*(2), 175-194. https://doi.org/10.1177/002199838101500207

Jiang, Y., & Wang, Q. (2016). Highly-stretchable 3D-architected mechanical metamaterials. *Scientific reports*, *6*(1), 34147. https://doi.org/10.1038/srep34147

Kebadze, E., Guest, S., & Pellegrino, S. (2004). Bistable prestressed shell structures. *International Journal of Solids and Structures*, *41*(11-12), 2801-2820. https://doi.org/10.1016/j.ijsolstr.2004.01.028

Khan, M., Baig, T., & Mirza, S. (2012). Experimental investigation of in-plane and out-of-plane crushing of aluminum honeycomb. *Materials Science and Engineering: A*, *539*, 135-142. https://doi.org/10.1016/j.msea.2012.01.070

Khosroshahi, S. F., Tsampas, S., & Galvanetto, U. (2018). Feasibility study on the use of a hierarchical lattice architecture for helmet liners. *Materials Today Communications*, *14*, 312-323. https://doi.org/10.1016/j.mtcomm.2018.02.002

Kooistra, G. W., & Wadley, H. N. (2007). Lattice truss structures from expanded metal sheet. *Materials & Design*, *28*(2), 507-514. https://doi.org/10.1016/j.matdes.2005.08.013

Kuang, Z., Huang, Q., Huang, W., Yang, J., Zahrouni, H., Potier-Ferry, M., & Hu, H. (2021). A computational framework for multi-stability analysis of laminated shells. *Journal of the Mechanics and Physics of Solids*, *149*, 104317. https://doi.org/10.1016/j.jmps.2021.104317

Kucewicz, M., Baranowski, P., & Małachowski, J. (2019). A method of failure modeling for 3D printed cellular structures. *Materials & Design*, *174*, 107802. https://doi.org/10.1016/j.matdes.2019.107802

Lachenal, X., Daynes, S., & Weaver, P. M. (2013). Review of morphing concepts and materials for wind turbine blade applications. *Wind energy*, *16*(2), 283-307. https://doi.org/10.1002/we.531

Li, H., Dai, F., Weaver, P., & Du, S. (2014). Bistable hybrid symmetric laminates. *Composite Structures*, *116*, 782-792. https://doi.org/10.1016/j.compstruct.2014.05.030

Liu, J., Chen, T., Zhang, Y., Wen, G., Qing, Q., Wang, H., Sedaghati, R., & Xie, Y. M. (2019). On sound insulation of pyramidal lattice sandwich structure. *Composite Structures*, *208*, 385-394. https://doi.org/10.1016/j.compstruct.2018.10.013

Liu, T.-W., Bai, J.-B., Xi, H.-T., Fantuzzi, N., Bu, G.-Y., & Shi, Y. (2023). Experimental and numerical investigation on folding stable state of bistable deployable composite boom. *Composite Structures*, *320*, 117178. https://doi.org/10.1016/j.compstruct.2023.117178

Liu, T., Bai, J., & Fantuzzi, N. (2024). Analytical model for predicting folding stable state of bistable deployable composite boom. *Chinese Journal of Aeronautics*, *37*(8), 460-469. https://doi.org/10.1016/j.cja.2023.05.021

Mattioni, F., Weaver, P. M., & Friswell, M. (2009). Multistable composite plates with piecewise variation of lay-up in the planform. *International Journal of Solids and Structures*, *46*(1), 151-164. https://doi.org/10.1016/j.ijsolstr.2008.08.023

Mukherjee, A., Friswell, M. I., Ali, S. F., & Arockiarajan, A. (2020). Modeling and design of a class of hybrid bistable symmetric laminates with cantilever boundary configuration. *Composite Structures*, *239*, 112019. https://doi.org/10.1016/j.compstruct.2020.112019

Nagesha, B., Dhinakaran, V., Shree, M. V., Kumar, K. M., Chalawadi, D., & Sathish, T. (2020). Review on characterization and impacts of the lattice structure in additive manufacturing. *Materials Today: Proceedings*, *21*, 916-919. https://doi.org/10.1016/j.matpr.2019.08.158

Nečemer, B., Glodež, S., Novak, N., & Kramberger, J. (2020). Numerical modelling of a chiral auxetic cellular structure under multiaxial loading conditions. *Theoretical and Applied Fracture Mechanics*, *107*, 102514. https://doi.org/10.1016/j.tafmec.2020.102514

Pan, D., Wu, Z., Dai, F., & Tolou, N. (2020). A novel design and manufacturing method for compliant bistable structure with dissipated energy feature. *Materials & Design*, *196*, 109081. https://doi.org/10.1016/j.matdes.2020.109081

Queheillalt, D. T., Murty, Y., & Wadley, H. N. (2008). Mechanical properties of an extruded pyramidal lattice truss sandwich structure. *Scripta Materialia*, *58*(1), 76-79. https://doi.org/10.1016/j.scriptamat.2007.08.041

Rafsanjani, A., Akbarzadeh, A., & Pasini, D. (2015). Snapping Mechanical Metamaterials under Tension. *Advanced Materials*, *27*(39), 5931-5935. https://doi.org/10.1002/adma.201502809

Rafsanjani, A., & Pasini, D. (2016). Bistable auxetic mechanical metamaterials inspired by ancient geometric motifs. *Extreme Mechanics Letters*, *9*, 291-296. https://doi.org/10.1016/j.eml.2016.09.001

Risso, G., Sakovsky, M., & Ermanni, P. (2022). A Highly Multi-Stable meta-structure via anisotropy for large and reversible shape transformation. *Advanced Science*, *9*(26), 2202740. https://doi.org/10.1002/advs.202202740

Shan, S., Kang, S. H., Raney, J. R., Wang, P., Fang, L., Candido, F., Lewis, J. A., & Bertoldi, K. (2015). Multistable Architected Materials for Trapping Elastic Strain Energy. *Advanced Materials*, *27*(29), 4296-4301. https://doi.org/10.1002/adma.201501708

Spadoni, A., & Ruzzene, M. (2007). Numerical and experimental analysis of the static compliance of chiral truss-core airfoils. *Journal of Mechanics of Materials and Structures*, *2*(5), 965-981. https://doi.org/10.2140/jomms.2007.2.965

Tancogne-Dejean, T., & Mohr, D. (2018). Elastically-isotropic truss lattice materials of reduced plastic anisotropy. *International Journal of Solids and Structures*, *138*, 24-39. https://doi.org/10.1016/j.ijsolstr.2017.12.025

Tancogne-Dejean, T., Diamantopoulou, M., Gorji, M. B., Bonatti, C., & Mohr, D. (2018). 3D plate-lattices: an emerging class of low-density metamaterial exhibiting optimal isotropic stiffness. *Advanced Materials*, *30*(45), 1803334. https://doi.org/10.1002/adma.201803334

Udani, J. P., & Arrieta, A. F. (2021). Programmable mechanical metastructures from locally bistable domes. *Extreme Mechanics Letters*, *42*, 101081. https://doi.org/10.1016/j.eml.2020.101081

Vidoli, S., & Maurini, C. (2008). Tristability of thin orthotropic shells with uniform initial curvature. *Proceedings of the Royal Society A: Mathematical, Physical and Engineering Sciences*, *464*(2099), 2949-2966. https://doi.org/10.1098/rspa.2008.0094

Waitukaitis, S., Menaut, R., Chen, B. G.-g., & Van Hecke, M. (2015). Origami multistability: from single vertices to metasheets. *Physical review letters*, *114*(5), 055503. https://doi.org/10.1103/PhysRevLett.114.055503

Wang, B., Wu, L., Ma, L., Sun, Y., & Du, S. (2010). Mechanical behavior of the sandwich structures with carbon fiber-reinforced pyramidal lattice truss core. *Materials & Design (1980-2015)*, *31*(5), 2659-2663. https://doi.org/10.1016/j.matdes.2009.11.061

Wang, C., Li, Y., Zhao, W., Zou, S., Zhou, G., & Wang, Y. (2018). Structure design and multi-objective optimization of a novel crash box based on biomimetic structure. *International Journal of Mechanical Sciences*, *138*, 489-501. https://doi.org/10.1016/j.ijmecsci.2018.01.032

Yang, Y., Dias, M. A., & Holmes, D. P. (2018). Multistable kirigami for tunable architected materials. *Physical Review Materials*, *2*(11), 110601. https://doi.org/10.1103/PhysRevMaterials.2.110601

Yasuda, H., & Yang, J. (2015). Reentrant origami-based metamaterials with negative Poisson's ratio and bistability. *Physical review letters*, *114*(18), 185502. https://doi.org/10.1103/PhysRevLett.114.185502

Yin, H., Liu, Z., Dai, J., Wen, G., & Zhang, C. (2020). Crushing behavior and optimization of sheet-based 3D periodic cellular structures. *Composites Part B: Engineering*, *182*, 107565. https://doi.org/10.1016/j.compositesb.2019.107565

Zhang, D., Lu, G., Ruan, D., Fei, Q., & Duan, W. (2019). Quasi-static combined compression-shear crushing of honeycombs: An experimental study. *Materials & Design*, *167*, 107632. https://doi.org/10.1016/j.matdes.2019.107632

Zhang, L., Chen, Y., He, R., Bai, X., Zhang, K., Ai, S., Yang, Y., & Fang, D. (2020). Bending behavior of lightweight C/SiC pyramidal lattice core sandwich panels. *International Journal of Mechanical Sciences*, *171*, 105409. https://doi.org/10.1016/j.ijmecsci.2019.105409

Zhang, L., Hu, Z., Wang, M. Y., & Feih, S. (2021). Hierarchical sheet triply periodic minimal surface lattices: design, geometric and mechanical performance. *Materials & Design*, *209*, 109931. https://doi.org/10.1016/j.matdes.2021.109931

Zhang, X., Ma, J., Li, M., You, Z., Wang, X., Luo, Y., Ma, K., & Chen, Y. (2022). Kirigami-based metastructures with programmable multistability. *Proceedings of the National Academy of Sciences*, *119*(11), e2117649119. https://doi.org/10.1073/pnas.2117649119

Zhang, Y., Wang, Q., Tichem, M., & van Keulen, F. (2020). Design and characterization of multi-stable mechanical metastructures with level and tilted stable configurations. *Extreme Mechanics Letters*, *34*, 100593. https://doi.org/10.1016/j.eml.2019.100593

Zhang, Z., Lou, C., Liang, Y., & Pan, D. (2024). Bistable hybrid symmetric laminates with a clamped-clamped boundary condition: An experimental and numerical investigation. *Composite Structures*, *327*, 117654. https://doi.org/10.1016/j.compstruct.2023.117654

Zhao, M., Zhang, D. Z., Liu, F., Li, Z., Ma, Z., & Ren, Z. (2020). Mechanical and energy absorption characteristics of additively manufactured functionally graded sheet lattice structures with minimal surfaces. *International Journal of Mechanical Sciences*, *167*, 105262. https://doi.org/10.1016/j.ijmecsci.2019.105262

Zheng, X., Smith, W., Jackson, J., Moran, B., Cui, H., Chen, D., Ye, J., Fang, N., Rodriguez, N., & Weisgraber, T. (2016). Multiscale metallic metamaterials. *Nature materials*, *15*(10), 1100-1106. https://doi.org/10.1038/nmat4694